Reingestion Characteristics and Inlet Flow Distortion of V/STOL Lift-Engine Fighter Configurations

JERRY V. KIRK* AND JERRY P. BARRACK*
NASA Ames Research Center, Moffett Field, Calif.

Short path reingestion of exhaust gas into engine inlets during hover with high-temperature rise and inlet flow distortion during transition are two important problem areas for lift-engine powered V/STOL aircraft. These problems have been studied at NASA Ames Research Center using a large-scale generalized lift-engine fighter model powered by J-85 engines. The factors affecting exhaust gas reingestion, engine surge, and hover performance are presented and discussed for two lift-engine arrangements. Inlet flow distortion and total pressure recovery during transition from hover to wing supported flight are shown for both lift-engine configurations. Excessive thrust loss and compressor stalls were experienced when the exhaust vector angle was 90°. Vectoring the exhaust approximately ±20° from vertical virtually eliminated reingestion. VTOL operation does appear promising with the lift engines vectored forward and the lift-cruise engines aft to balance the aircraft and alleviate exhaust gas reingestion. Inlet flow distortion and total pressure recovery were within acceptable limits for the engines used under most test conditions.

Nomenclature

D = inlet or exit diameter, in.
F_g = engine gross thrust, lb
H = height from ground plane to fuselage reference, in.
N = inlet pressure distortion, $(P_{t_{max}} - P_{t_{min}})/P_{t_{av}}$
P = pressure, psi
P_3/P_2 = ratio of compressor discharge pressure to compressor inlet pressure
q = dynamic pressure, $(\frac{1}{2})\rho V^2$, psf
Q = temperature distortion, $(T_{max} - T_{min})/T_{av}$, °R
r = radius, in.
T = temperature, °F or °R
ΔT = temperature rise above ambient, °F
V = velocity, fps
W = fuselage width
α = angle of attack, deg
β = angle of sideslip, deg
η = angle between the engine axis and the swivel axis, deg
ρ = density, lb/ft³
σ = angle between engine axis and the horizontal measured in a plane perpendicular to the swivel axis, deg

Subscripts

av = average
e = exit
i = inlet
max = maximum
min = minimum
0 = freestream
s = static
T = total

Introduction

PAST research[1-4] has shown that reingestion of exhaust gas and flow distortion in the lift-engine inlet are major problems during transition for lift-engine powered V/STOL aircraft. The first, caused by reingestion of exhaust gases, is at best a reduction in performance and at worst engine compressor surge. Work reported in Refs. 1 and 4 evaluated the effect of aircraft configuration on reingestion. This paper will discuss the efforts to reduce ingestion on an aircraft configuration. Reference 1 indicated that the second problem airflow distortion at the lift-engine compressor face, was largely eliminated by an inlet with a radius-to-diameter ratio of 0.56 and the engine tilted 10°. Since these dimensions result in a rather bulky installation, recent research at Ames has been directed toward achieving an acceptable inlet flow with vertical engines and a smaller inlet radius for application to a supersonic fighter aircraft.

These two problems have been studied at Ames Research Center on a large-scale lift-engine powered aircraft representative of a variable-sweep fighter. Results from the Ames hover test facility will be presented showing inlet temperature rise and temperature gradients for different exhaust vector angles and ground heights. Minor modifications to the model to alleviate the reingestion problem will be discussed.

Results from investigation in the Ames 40- by 80-ft wind tunnel to determine inlet flow distortion, and inlet total pressure recovery will be presented. The effects of an inlet vane and engine tilt will be shown for a range of flight speeds, power settings, and airplane angles of attack.

Model and Instrumentation

The model had a high wing and was representative of a variable-sweep fighter aircraft. The lift engines (J-85 turbojets) were located in two different positions (Fig. 1). The first configuration had four swiveling, retractable engines mounted at the sides of the fuselage. The engines were swiveled to give exhaust vector angles σ from 30° to 110°. Tests were conducted with the engines in two swivel planes as shown in Fig. 1. Engine toe out angles η up to 15° were available in both swivel planes. The second configuration had three internally fixed in-line engines installed vertically in the forward fuselage. For this configuration, ingestion characteristics were obtained with three different exit nozzles (Fig. 2).

Both configurations had two lift-cruise engines installed in the aft fuselage with the inlets above the wing. An inlet duct extension was added to the inlets during the tests with the swiveling, retractable lift engines. Figure 3 is a sketch of the inlet for the swiveling, retractable lift engine. A circular inlet vane was placed around the forward half of the internally fixed lift-engine inlets (Fig. 4) to help turn the flow into the vertically mounted engines during transition.

Presented as Paper 68-78 at the AIAA 6th Aerospace Sciences Meeting, New York, January 22–24, 1968; submitted January 22, 1968; revision received September 26, 1968.

* Research Scientists, Full-Scale and Systems Research Division.

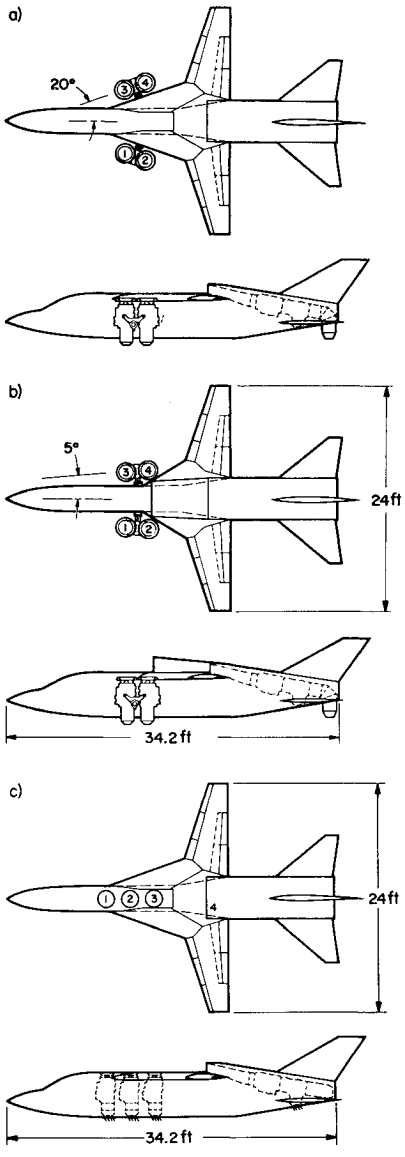

Fig. 1 General arrangement of the model—a) swiveling, retractable engines, 20° swivel plane, no duct extension, b) swiveling, retractable engines, 5° swivel plane, duct extension installed, and c) internally fixed lift engines.

Reingestion Instrumentation

Each of the four lift-engine inlets of the swiveling, retractable configuration had 12 thermocouples, whereas the three inlets of the internally fixed lift engines had 16. The left-hand lift-cruise engine was instrumented at the compressor face with 16 thermocouples. When the duct extension was

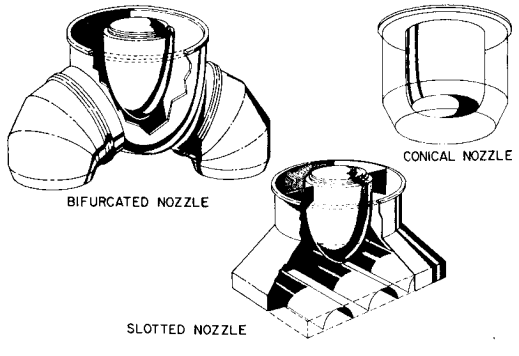

Fig. 2 Exit nozzles tested with internally fixed lift-engine configuration.

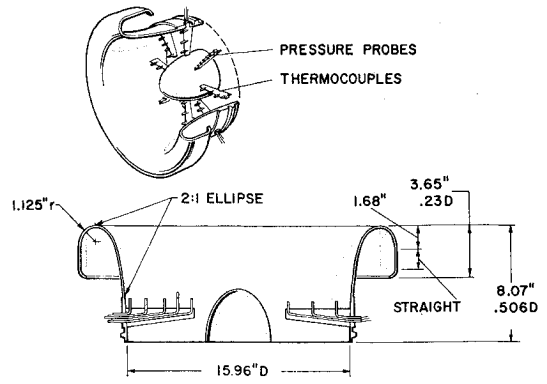

Fig. 3 Inlet for swiveling, retractable lift engines.

installed (swiveling, retractable configuration only), nine thermocouples were installed at the inlet plane.

Evaluating exhaust gas reingestion temperature gradients and absolute temperatures is complicated by changes that occur at rates higher than existing thermocouples can measure. High-response thermocouples must be small with very low thermal mass. These requirements place restrictions on thermocouples that are inconsistent with life and reliability. The thermocouples used in this investigation were iron-constantan wire, 0.005 and 0.010 in. in diameter. These wire sizes have time constants of 30 to 100 msec. Although relatively fast, these thermocouples are inadequate for measuring the abrupt temperature gradients experienced; however, it is possible to reconstruct the actual input temperature history, given the output temperature history and tepmerature pickup response characteristics.

Pressure Distortion Instrumentation

Sixteen total pressure tubes were placed in each lift-engine inlet and the left-hand lift-cruise engine inlet for measuring inlet distortion and total pressure recovery during transition for both configurations.

Results and Discussion

Exhaust Gas Reingestion

Two distinct types of exhaust gas reingestion occur in lift-engine powered V/STOL configurations. The first type is characterized by exhaust flow spreading along the ground some distance from the aircraft. After it loses most of its velocity, this gas, because of its bouyant nature, eventually circulates back to the engine inlets. Because this exhaust gas mixes with ambient air, the temperature at the inlet rises only a few degrees above the ambient air temperature.

The second type of exhaust gas reingestion is a short-path, high-temperature rise reingestion caused by a high-velocity exhaust jet meeting another exhaust jet flowing in the opposite direction. The result is an upward flow of high-temperature

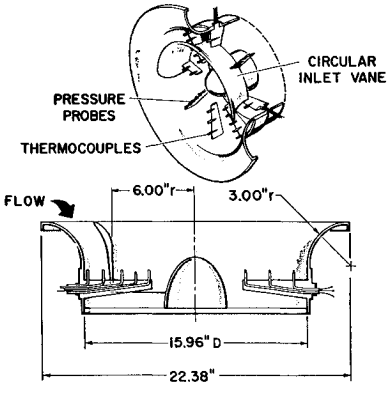

Fig. 4 Inlet for internally fixed lift engines.

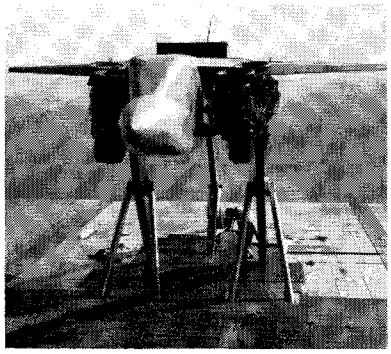

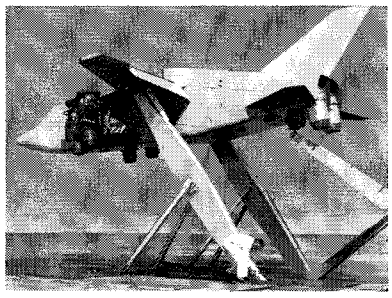

Fig. 5 Photograph of model with swiveling, retractable lift engines mounted on Ames static test stand.

gases that have little opportunity to mix with the ambient air. They usually enter the engine inlet in a localized region and can cause the engine to stall. This type of ingestion will be discussed in this presentation.

Flow Patterns

The swiveling, retractable lift-engine configuration, photographs of which are shown in Fig. 5, had two distinct fountains of hot exhaust beneath the model. One fountain formed under the fuselage between the lift engines (Fig. 6a) and the second fountain formed where the exhaust gases from the lift engines flowing aft met the forward flowing exhaust from the lift-cruise engines. The first fountain rose on either side of the fuselage between the fuselage and lift engines to the vicinity of the inlets while the second fountain was deflected by the wing and also channeled into the vicinity of the lift-engine inlets. Swiveling the lift-engines and lift-cruise engines $\pm 20°$ from vertical changed the location of the fountains. Placing doors on the lower side of the fuselage between the fuselage and the lift engines reduced the upward flow of hot exhaust gases from the forward fountain; however, exhaust flowing around the doors (all results shown are with these doors) meeting the high-temperature turbulent flow

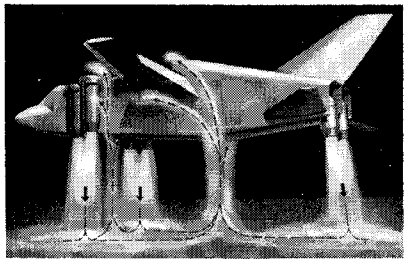

a) Swiveling, retractable configuration.

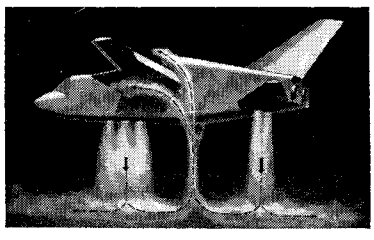

b) Internally fixed configuration.

Fig. 6 Short-path, high-temperature rise flow patterns.

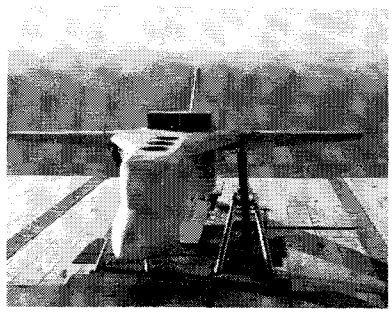

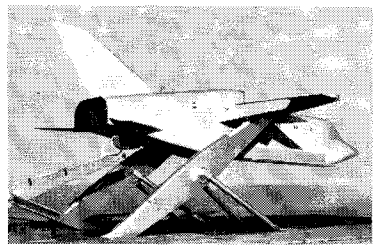

Fig. 7 Photograph of model with internally fixed lift engines showing location of doors.

from the rear fountain was still channeled by the wing into the vicinity of the lift-engine inlets.

With the internally fixed configuration the exhaust gases were vectored from vertical to 20° aft with three separate exhaust nozzles (conical, bifurcated, and slotted) at each ground height. Some studies were done with doors placed along the bottom of the fuselage to break up the short path recirculation of hot exhaust gases. Figure 7 is a photograph of the model at the test facility showing the location of the doors. The three lift-engines of the internally fixed configuration were close together so that the exhaust coalesced to form a single sheet of hot exhaust. This exhaust flowing aft joined the forward flowing exhaust from the lift-cruise engines. The rising turbulent flow was channeled by the under surface of the wing and wing leading-edge strake into the vicinity of the lift-engine inlets (Fig. 6b).

Test Results

A general summary of the ingestion results obtained for both the swiveling, retractable and internally fixed lift-engine configurations shows (Fig. 8) the effects of exhaust gas vectoring. Only the swiveling, retractable configuration could be vectored forward (90° to 110°). Of the four ground heights tested (2.5, 5.0, 7.5, and 9.7), height-diameter ratios between 5 and 7.5 were the worst for ingestion. Results shown are general and are for a no-wing condition. The engine toe out angle for the swiveling, retractable lift engines was 15°, but the results at 0° are similar. Of the three exhaust nozzles tested with the internally fixed lift engines, the slotted nozzle produced somewhat lower-temperature gradients and average inlet temperatures than the conical or bifurcated nozzles;

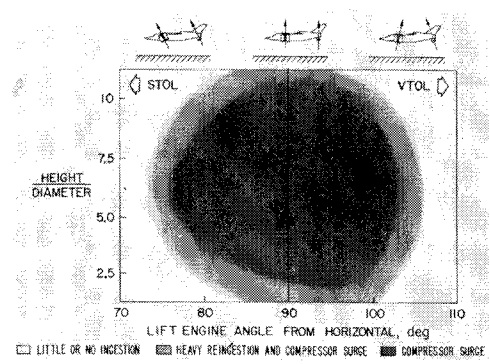

Fig. 8 General operating boundaries for lift-engine fighter model.

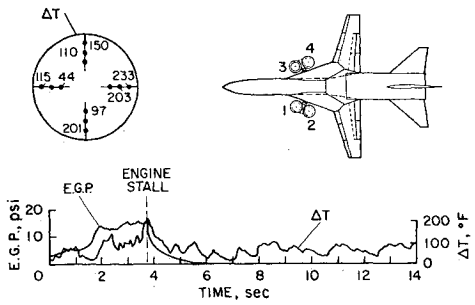

Fig. 9 Time-temperature history of configuration with high ingestion; swiveling, retractable engines 90° from horizontal, H/D = 5.0, no duct extension.

however, with exhaust vector angles of 80° and 90° the engines stalled regardless of exhaust nozzle installation.

No forward vectoring (90° to 110°) was accomplished with the internally fixed configuration, due to limitation in the thrust vectoring system. Nevertheless, there is no reason to believe, because of the similarity between 70° and 90°, that the results would be different from those shown for the swiveling, retractable configuration. Proper vectoring of the lift engines forward and lift-cruise engines aft to balance moment, provided thrust-to-weight ratios were adequate, should provide VTOL capability to both configurations.

Figures 9–11 show results for the lift engines of the swiveling, retractable lift-engine configuration. All the results are shown for a height-diameter ratio of 5.0. Figure 9 shows the time-temperature history of the number 4 engine with the

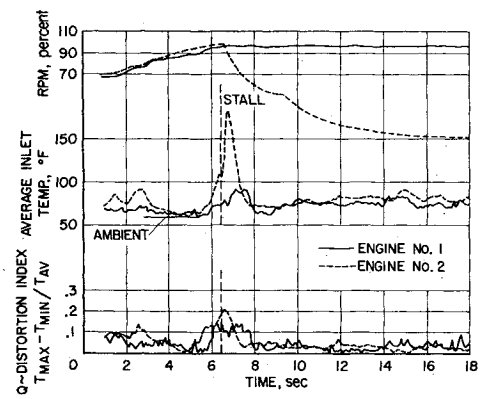

a) Lift engines 100° from horizontal, lift-cruise engines 80° from horizontal.

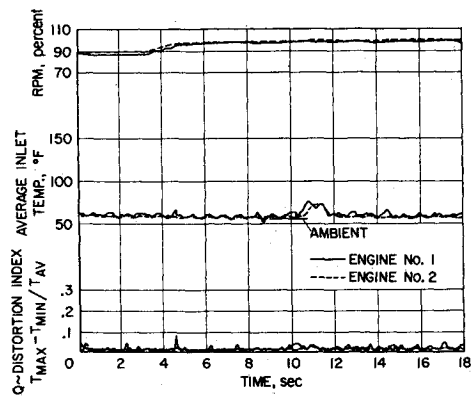

b) Lift engines 70° from horizontal, lift-cruise engines 80° from horizontal.

Fig. 10 Average inlet temperature and temperature distortion; swiveling, retractable configuration, H/D = 5.0, duct extension installed.

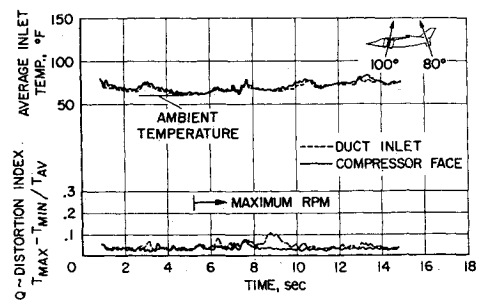

Fig. 11 Effect of inlet duct extension on average temperature and temperature distortion on left lift-cruise engine; lift engines 100° from horizontal, lift-cruise engines 80° from horizontal, H/D = 5.0.

vector angle at 90° and the engines in the 20° swivel plane. Only one thermocouple is shown to depict the extremely turbulent temperature conditions. The thermocouple chosen was that which showed the largest transients. The exhaust gas pressure (EGP) is also superimposed on the trace. In this case the engine stalled at $3\frac{1}{2}$ sec on the time scale. Measured average inlet temperature rise was 144° with maximum temperature gradients on the order of 1000°/sec. When corrected for thermocouple response, using the method reported in Ref. 4, these figures are 157° and 1700°/sec. The highest temperature rise was measured near the outer circumference of the compressor face at 3:00 and 6:00 o'clock positions on the engine.

Measured average inlet temperature (corrected for thermocouple response) and distortion index are shown in Fig. 10 for the swiveling, retractable lift engines in the 5° swivel plane with the lift-cruise engine duct extension installed. Figure 10a is an example of high ingestion (lift engine σ = 100°, lift-cruise engine σ = 80°). Average inlet temperature in the engine 2 approaches 200°F (ΔT = 125°) during engine stall and backfire. The distortion index at stall is approximately 0.2. Results are shown at the same ground height for a configuration with low ingestion in Fig. 10b. In this figure, the lift-engine swivel angle was 70° while the lift-cruise engine exhaust was vectored 80°. The average temperature rise in both inlets was less than 10° for the first 6 sec after maximum rpm was reached with the maximum temperature rise less than 20° for the entire run. The distortion index was less than 0.1 for the entire run.

Very few stalls occurred in the lift-cruise engines both with and without the duct extension and regardless of lift-engine vector angle. The wing apparently offered sufficient protection for the lift-cruise engine inlets. The duct did, however, act as a mixing chamber for the air entering the lift-cruise engines. Figure 11 presents the average temperature and temperature distortion index at the duct inlet and at the compressor face of the left-hand lift-cruise engine. The lift engines were swiveled to 100° and the lift-cruise engine exhaust vectored to 80°. Distortion levels above 0.1 were measured at the duct inlet while the maximum distortion

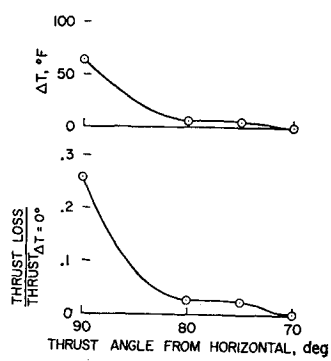

Fig. 12 Effect of thrust vectoring; swiveling, retractable configuration, H/D = 5.0.

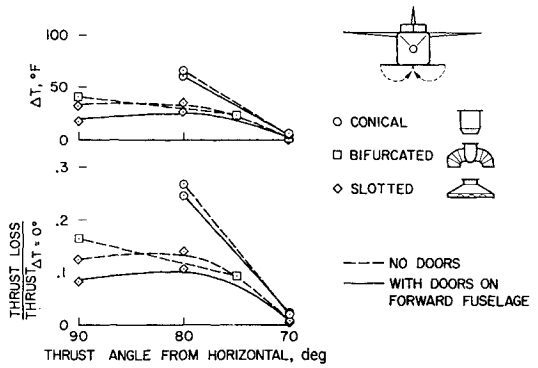

Fig. 13 Effect of thrust vectoring and doors on lower fuselage; internally fixed configuration, $H/D = 5.0$.

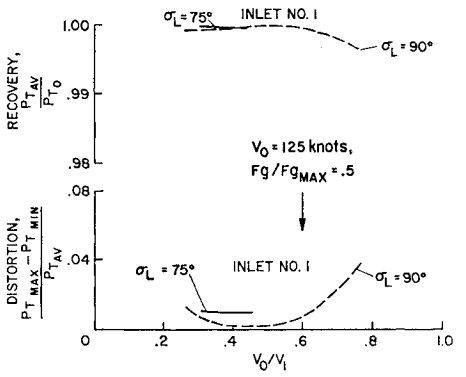

Fig. 15 Effect of velocity ratio on inlet flow distortion and pressure recovery; swiveling, retractable configuration.

level measured at the compressor face was approximately 0.08. With a measured maximum temperature rise of approximately 20°F, the average inlet temperatures at both the duct inlet and the compressor face were approximately equal in magnitude.

The effect of exhaust gas vectoring on thrust loss is shown in Fig. 12. The results presented are for a height-diameter ratio of 5.0, but similar results differing only in magnitude could be presented for other ground heights tested. The average inlet temperature increase of approximately 60° shown for the engines at 90° swivel angle represents a thrust loss on the order of 25% based on a 4% thrust loss for each 10° rise in average inlet temperature for the J-85 engine. As the engines were swiveled away from 90°, the inlet temperature rise decreased rapidly, resulting in a corresponding decrease in thrust loss, until at 70° swivel angle little or no thrust degradation was measured. The ratio shown was based on temperature measurements only and does not include induced aerodynamic effects. For a configuration such as the swiveling, retractable lift-engine fighter model, even if engines can be designed to tolerate the temperature increase shown for vertical engine operation without stalling, this exhaust would be vectored to avoid the thrust loss due to the temperature increase.

As with the swiveling, retractable configuration, exhaust gas vectoring was the most effective means of reducing or eliminating ingestion and the attendant thrust loss for the internally fixed lift-engine configuration. Results with gas vectoring are shown in Fig. 13 for the three exit nozzles used. The effect of placing doors on the bottom of the fuselage is also shown for the conical and slotted exit nozzles. Since it was not possible to operate the engines continuously at 80° and 90°, the results shown on the figure depend on engine modifications to provide stall-free operation. The ingestion level was lower with the slotted nozzles than with either the bifurcated or conical nozzles at all ground positions tested. Depending on the type of vectoring system used, doors along the bottom of the fuselage that could be used to seal the underside of the fuselage during conventional flight could, if properly placed, be effective in reducing the magnitude of the temperature increase.

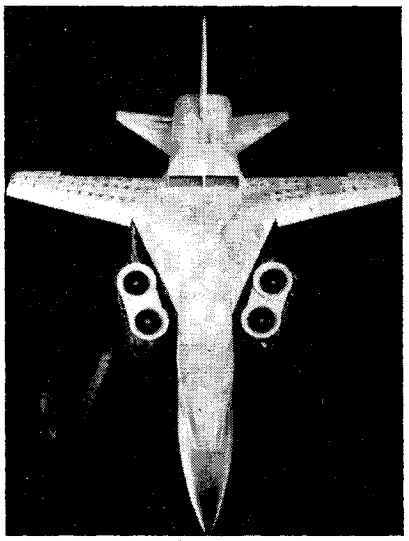

Fig. 14 Photograph of swiveling, retractable configuration mounted in the Ames 40- by 80-ft wind tunnel.

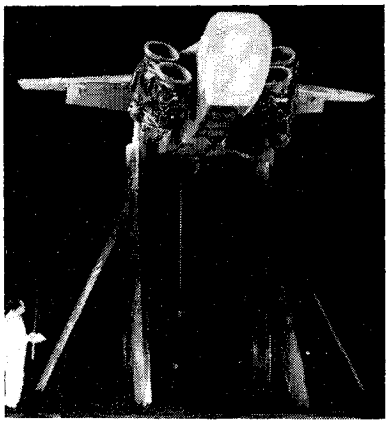

Inlet Performance in Transition

Inlet flow distortion and pressure recovery as well as exhaust gas reingestion are of primary concern for aircraft using lift engines for VTOL maneuvering. Flow distortion and inlet recovery were studied in the 40- by 80-ft wind tunnel during transition from hover to wing-supported flight for both lift-engine configurations.

Swiveling, Retractable Configuration

Figure 14 shows the model mounted in the wind tunnel. Engine thrust and wind-tunnel speed were varied for engine

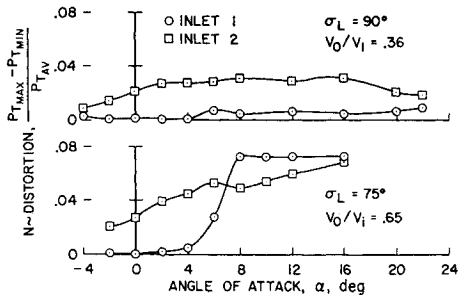

Fig. 16 The variation in flow distortion with angle of attack; swiveling, retractable configuration.

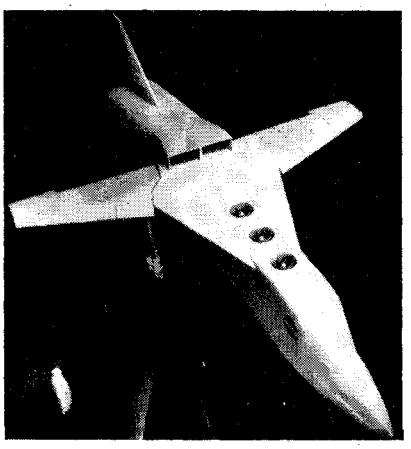

Fig. 17 Photograph of the internally fixed lift-engine configuration mounted in the 40- by 80-foot wind tunnel.

angles of 30° to 90° from horizontal. These conditions effectively simulated the full-scale flight conditions required to define both take-off and landing transitions adequately. A particular advantage of the swiveling, retractable configuration is that engine starting and acceleration at the beginning of a decelerating transition will not impose a severe inlet design condition on the lift engines. The engines can be rotated into the airstream at the beginning of the transition for starting, thereby eliminating the high crossflow angle and the necessity of the inlet decelerating the crossflow and turning this flow 90°. Once started, the engines can be accelerated and rotated toward the vertical position as the transition proceeds.

Test results indicate that the inlet used (Fig. 3) was acceptable throughout the velocity range and engine angles used during transition. The effect of inlet velocity ratio (the ratio of freestream to inlet velocity) on distortion and pressure recovery is shown for engine angles of 90° and 75° for the engine 1 inlet in Fig. 15. Maximum inlet distortion is less than 4% with inlet pressure recovery greater than 0.995. As engine angle was decreased toward horizontal, inlet distortion decreased until at an engine angle of 30°, there was little measurable distortion. The effect of angle of attack is shown in Fig. 16. Engine angles of 90° and 75° are shown. Distortion levels are within acceptable limits for the J-85 engine (less than 10%). The effect of sideslip angle on the variations of distortion and pressure recovery was negligible for sideslip angles of ±12° at all engine angles and inlet velocity ratios.

Internally Fixed Configuration

Figure 17 is a photograph of the internally fixed lift-engine configuration mounted in the 40- by 80-ft wind tunnel. The lift-engine inlets had a constant 3-in. radius (0.19 radius-to-inlet diameter ratio). Because of the relatively small radius, a circular inlet vane was placed in the forward 180° sector of the inlet to assist in turning the flow into the engine with increasing velocity ratios.

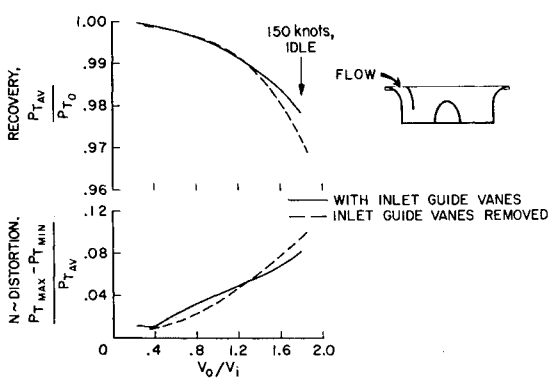

Fig. 18 Effect of velocity ratio on flow distortion and inlet recovery.

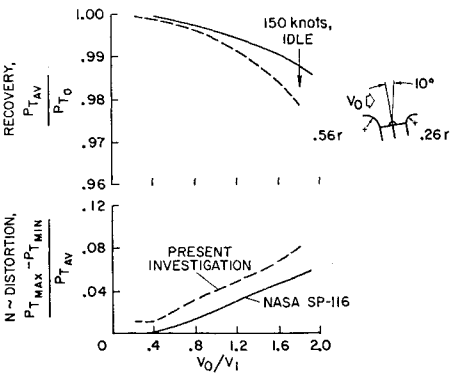

Fig. 19 Comparison of results between present investigation and Ref. 1; inlet number 1.

The effect of velocity ratio on inlet distortion and pressure recovery with and without the inlet guide vanes installed is shown in Fig. 18. Comparison shows that at a velocity ratio of 1.8 (corresponding to 150 knots forward speed with the engines at idle thrust), the distortion level was decreased approximately 2% with the inlet guide vane installed; however, distortion levels were within acceptable limits for the J-85 in both instances. The effect of velocity ratio on distortion and pressure recovery for a model previously reported on is shown in Fig. 19. The engines were tilted 10° aft of vertical. This allowed a generous leading-edge inlet radius (0.56 radius-to-inlet diameter ratio). Comparison of these results with the model of this investigation with the inlet guide vane installed shows, as expected, somewhat better pressure recovery and slightly lower distortion levels at the high velocity ratios; however, the distortion levels from both investigations were well below the nominal acceptable level of 10%.

Figure 20 shows the variation in distortion with angle of attack for relatively high velocity ratios, with and without the inlet guide vanes installed. With the guide vanes installed, the variation in distortion levels and inlet recovery was negligible. Comparison shows that with the inlet guide vane removed the distortion level is approximately 2% higher and the variation in distortion is also more pronounced. At a velocity ratio of 1.85 the nominal acceptable distortion level of 10% is exceeded in inlet 1, regardless of angle of attack. The trends were similar when sideslip angle was varied. With the inlet guide vanes installed, distortion and recovery levels were fairly constant with change in sideslip angle. With the inlet guide vanes removed, distortion levels were on the order of 2% higher. As with angles of attack, the variation in distortion was more pronounced with the guide vane removed.

Summary and Results

The results presented show:

1) Excessive thrust loss and compressor stalls were experienced with both the swiveling, retractable and internally

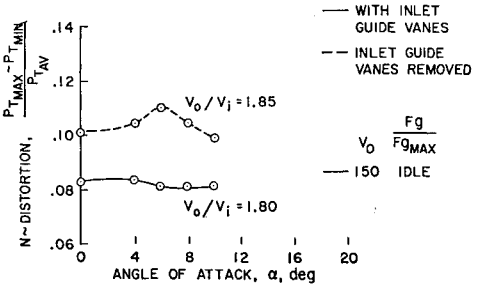

Fig. 20 The variation in flow distortion with angle of attack; internally fixed configuration, inlet number 1.

fixed lift-engine configurations when the exhaust vector angle was 90° from horizontal. Vectoring the exhaust to 70° (or 110° in the case of the swiveling, retractable configuration) virtually eliminated reingestion.

2) Vertical engine operation with a configuration like the model tested does not appear to be feasible. Even if engines can be built to withstand temperature rise and temperature distortion of the magnitude shown, the loss in thrust resulting from the temperature rise would greatly reduce mission capability.

3) VTOL operation does appear promising with the lift engines vectored forward and the lift-cruise exhaust aft to balance the aircraft and alleviate exhaust gas reingestion. The aircraft could then take off and land within an area surrounded by hot exhaust but be relatively free from ingestion effects.

4) Inlet flow distortion and total pressure recovery for the swiveling, retractable lift-engine configuration was well within acceptable limits for the engines used.

5) Pressure distortion for a 0.19 radius inlet with a vertical engine was within acceptable limits for the J-85 engine.

6) The circular inlet guide vane installed on the internally fixed lift-engine inlets was helpful in turning the flow into the engine at the higher velocity ratios. The distortion levels with angle of attack and angle of sideslip were approximately 2% lower with the inlet vane installed.

References

[1] Tolhurst, W. H. and Kelly, M. W., "Characteristics of Two Large-Scale Jet-Lift Propulsion Systems," SP-116, Paper 15, 1966, NASA.

[2] Lavi, R., "An Experimental Investigation of a VTOL Lift-Engine Inlet," *Journal of Aircraft*, Vol. 4, No. 2, March-April 1967, pp. 125–132.

[3] Tyson, B. I., "Tests to Establish Flow Distortion Criteria for Lift Engines," *Journal of Aircraft*, Vol. 2, No. 5, Sept.-Oct. 1965, pp. 411–417.

[4] Lavi, R., Hall, G. R., and Stark, W. W., "Full-Scale Ground Proximity Investigation of a VTOL Fighter Model Aircraft," NOR 67-221, 1967, Northrop Corp., Norair Div.